FIBROUS FOITITE FROM ŞEBİNKARAHİSAR, GİRESUN Pb–Zn–Cu–(U) MINERALIZED AREA, NORTHERN TURKEY

FUAT YAVUZ[1]

İstanbul Teknik Üniversitesi, Maden Fakültesi, Maden Yatakları-Jeokimya Anabilim Dalı, 80670, Maslak, İstanbul, Turkey

MUAZZEZ ÇELİK AND NECATİ KARAKAYA

*Selçuk Üniversitesi, Mühendislik Mimarlık Fakültesi, Jeoloji Mühendisliği Bölümü,
Mineraloji-Petrografi Anabilim Dalı, 42250, Konya, Turkey*

ABSTRACT

Fibrous foitite occurs in cavities in quartz veins near Şebinkarahisar town, Giresun mineralized area [Pb–Zn–Cu–(U)], in northern Turkey. Veins of quartz + fibrous tourmaline generally cut monzonitic and syenitic rocks. Acicular and hairlike light gray crystals of foitite have a mean composition of $\square_{0.43}Na_{0.52}Ca_{0.07}$ ($Fe_{1.55}Mn_{0.08}Mg_{0.52}$ $Al_{0.67}Ti_{0.01}$) Al_6 (BO_3)$_3$ Si_6 O_{18} (OH,O)$_3$ (OH)$_1$. The crystals of this low-temperature tourmaline radiate from irregular patches of schorl in cavities in quartz veins. Each fiber is zoned along its length with respect to Fe, Mn, Mg, Ca, Na, K, and P. The fibrous foitite from the Şebinkarahisar area contains higher Mg, Ca and Na contents than that from southern California and Elba.

Keywords: foitite, tourmaline, fibers, alkali-deficient, cavity, quartz vein, Pb–Zn–Cu–(U) mineralization, Şebinkarahisar, northern Turkey.

SOMMAIRE

On trouve des cristaux fibreux de foïtite dans des cavités de veines de quartz près de Şebinkarahisar, zone minéralisée de Giresun [Pb–Zn–Cu–(U)], dans le nord de la Turquie. Les veines de quartz + tourmaline fibreuse recoupent en général des roches monzonitiques ou syénitiques. Les cristaux aciculaires et capillaires gris pâle de foïtite ont une composition moyenne de $\square_{0.43}Na_{0.52}Ca_{0.07}$ ($Fe_{1.55}Mn_{0.08}Mg_{0.52}$ $Al_{0.67}Ti_{0.01}$) Al_6 (BO_3)$_3$ Si_6 O_{18} (OH,O)$_3$ (OH)$_1$. Il s'agit d'une tourmaline de basse température en amas fibro-radiés développés sur des taches irrégulières de schorl le long des parois de cavités dans des veines de quartz. Chaque fibre est zonée le long de la fibre par rapport à sa teneur en Fe, Mn, Mg, Ca, Na, K, et P. Les échantillons de foïtite fibreuse provenant de Şebinkarahisar contiennent plus de Mg, Ca et Na que les exemples connus du sud de la Californie et de l'île d'Elba.

(Traduit par la Rédaction)

Mots-clés: foïtite, tourmaline, fibres, déficit en alcalins, cavité, veine de quartz, minéralisation en Pb–Zn–Cu–(U), Şebinkarahisar, Turquie.

INTRODUCTION

Tourmaline presents a complex chemical spectrum owing to its extensive substitutions at the *X*, *Y*, and *Z* sites. The general formula of tourmaline is given as X Y_3 Z_6 (BO_3)$_3$ Si_6O_{18} (OH,O)$_3$ (OH,F,Cl,O), where $X =$ Na^+, Ca^{2+}, K^+, $\square$, $Y = Mg^{2+}$, Fe^{2+}, Mn^{2+}, Al^{3+}, Fe^{3+}, Mn^{3+}, Cr^{3+}, Li^+, $Z = Al^{3+}$, Mg^{2+}, Fe^{3+}, Cr^{3+}, V^{3+}. Alkali-deficient tourmaline is characterized by the predominance of vacancies at the *X* site (*i.e.*, $0 \le X_{total} < 0.5$). It seems that foitite is more common, but less strongly alkali-deficient, in ore-related environments than in pegmatite and aplite dikes (Foit *et al.* 1989).

Fibrous foitite was first described by Foit *et al.* (1989) as schorl with dumortierite in hydrothermally altered tuffs at Jack Creek, Jefferson County, Montana. Alkali-deficient tourmaline in this area occurs as irregular fibrous patches and cavity fillings in dumortierite-enriched rocks. MacDonald *et al.* (1993) described the highly alkali-deficient tourmaline (*i.e.*, $X_{total} = 0.26$) as

---

[1] *E-mail address*: yavuz@sariyer.cc.itu.edu.tr

foitite, and proposed the ideal composition $\square$ [Fe^{2+}_2 (Al,Fe^{3+})] Al_6 Si_6 O_{18} (BO_3)$_3$ (OH)$_4$ from an unknown locality in southern California. Pezzotta *et al.* (1996) defined a second occurrence of fibrous foitite from a complex pegmatite dike at San Piero in Campo, Elba, Italy.

In this study, we report on the occurrence of foitite from Şebinkarahisar, near the Giresun Pb–Zn–Cu–(U) mineralized area, in northern Turkey. The area investigated shows signs of widespread formation of tourmaline, hydrothermal alteration, Pb–Zn–Cu mineralization and, to a lesser extent, high-background radioactive anomalies of up to 40 ppm uranium (Çalapkulu 1982). Foitite from this area occurs as fragile acicular and hairlike crystals in cavities in quartz veins cutting Upper Cretaceous to Paleocene monzonitic plutonic rocks. We document here the mode of occurrence of the fibrous foitite and its compositional variations in relation to environment of mineralization.

MODE OF OCCURRENCE

The Asarcık plutonic rocks outcrop about 20 km north of the town of Şebinkarahisar, Giresun, in the eastern part of the Pontide metallogenic belt, in northern Turkey. The rocks in the study area range from alkali granite to diorite, but syenite, quartz syenite, monzonite, quartz monzonite, rhyolite, rhyodacite, and trachyandesite are dominant. In the study area, these rocks were separated into two groups, the lower and upper series (Çalapkulu 1982). The upper series is mainly composed of dacite, andesite, basalt and related tuffs and pyroclastic units. The lower series contains calcalkaline igneous rocks and interbedded sedimentary units. The upper series and part of the lower series are characterized by intensive formation of tourmaline, hydrothermal alteration and Pb–Zn–Cu mineralization. K–Ar age determinations by Oyman *et al.* (1995) on orthoclase, biotite and hornblende from the Asarcık suite and surrounding magmatic rocks indicate a time interval from Upper Cretaceous to Upper Paleocene (*i.e.*, 82.4 to 58.3 Ma). Monzonite, quartz monzonite and quartz syenite is cut by later quartz veins (1 to 15 cm) and aplite dikes up to 5 cm in thickness. These quartz veins contain cavities up to 2 cm across and about 1 cm in depth, especially around the Asarcık region. Black schorl, about 0.5 cm thick, rims these cavities. The light gray acicular and hairlike fibrous tourmaline crystals project inward from the schorl rim (Fig. 1). Pezzotta *et al.* (1996) pointed out that fibrous foitite from Elba only develops as an overgrowth on the analogous end of the tourmaline crystals. According to their study, the antilogous end of crystals is composed mainly of coarse-grained schorl–elbaite. In terms of their physical appearance, our samples of fibrous foitite from Şebinkarahisar show a great similarity to that at Elba except for the absence of dark brown antilogous schorl-elbaite ends. Figure 2a shows a SEM (scanning electron microscopy)

low-magnification view of a miarolitic cavity in a quartz vein. In this figure, the acicular and hairlike crystals radiate from the irregular patches of schorl in the foreground. A higher-magnification view of these acicular and hairlike crystals of fibrous tourmaline is shown in Figures 2b, c. Accessory minerals in the foitite-bearing quartz veins are K-feldspar, chrysoprase and hematite. Hematite is characteristic of an oxidized environment. Its presence may suggest Fe^{3+} in the structure of the coexisting tourmaline.

CHEMICAL COMPOSITION

Fibrous foitite-bearing samples in cavities of quartz veins were first cut into small sections for electron-microprobe determinations. In order to remove the dust and other impurities on fibrous tourmaline crystals, they were placed in an ultrasonic cleaner for a short time and then were carbon-coated for electron-microprobe studies. Microprobe analyses of samples were obtained by wavelength-dispersion spectrometry (WDS) at the laboratory of Metallurgy Engineering, Istanbul Technical University. A JEOL JSM–840 scanning microscope was used at 15 kV accelerating voltage, a beam current of 15 nA, a beam diameter of 5 μm, and a ZAF correction scheme. Representative electron-microprobe chemical data describing the fibrous tourmaline are given in Table 1. The TOURMAL software package (Yavuz 1997) was used for calculation and preparation of diagrams.

The mean chemical composition of the foitite is different than those described by MacDonald *et al.* (1993) and Pezzotta *et al.* (1996). The manganese contents of our tourmaline samples are low (0.18–1.32 wt.% MnO),
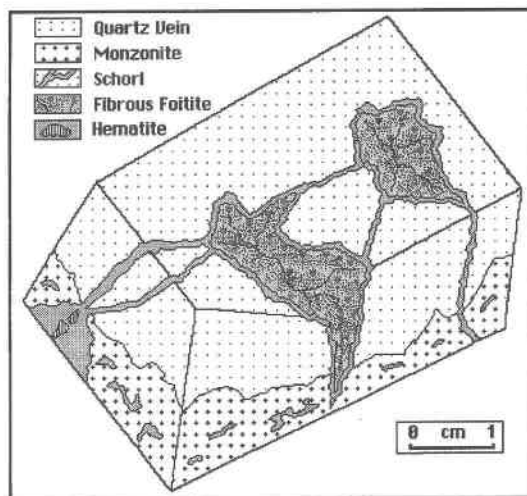

Fig. 1. Sketch of fibrous foitite samples in cavities in a quartz vein from Şebinkarahisar, Giresun, northern Turkey.

TABLE 1. REPRESENTATIVE RESULTS OF ELECTRON-MICROPROBE ANALYSES OF
ALKALI-DEFICIENT TOURMALINE (FOITITE) FROM ŞEBİNKARAHİSAR,
GİRESUN, NORTHERN TURKEY

	FOI -1	FOI -2	FOI -3	FOI -4	FOI -5	FOI -6	FIB -1	FIB -2	FIB -3	RIM -1	RIM -2	Şebin- karahisar	Elba (1)	Calif. (2)
SiO$_2$ wt%	35.64	35.53	35.75	35.82	35.87	35.52	36.16	35.78	36.43	32.35	33.09	35.68	36.09	35.90
Al$_2$O$_3$	32.96	34.30	33.71	33.97	33.77	33.20	32.76	35.08	34.41	30.08	31.66	33.65	34.91	34.90
TiO$_2$	0.00	0.08	0.00	0.00	0.11	0.11	0.00	0.00	0.00	0.17	0.10	0.05	0.09	0.00
FeO	11.96	11.53	11.12	10.58	10.75	10.39	10.66	9.34	6.23	18.71	15.59	11.05	10.93	11.45
MnO	0.85	0.47	0.53	0.18	0.20	1.32	0.93	0.18	0.16	0.70	0.73	0.59	1.36	1.71
MgO	1.56	1.37	1.80	2.75	2.29	2.76	1.58	1.64	4.67	2.86	3.22	2.08	0.33	0.21
CaO	0.52	0.32	0.53	0.21	0.41	0.38	0.39	0.22	0.19	0.51	0.70	0.39	0.03	0.03
Na$_2$O	1.52	1.55	1.58	1.61	1.70	1.53	2.27	2.37	2.41	1.48	1.58	1.58	1.11	0.75
K$_2$O	0.00	0.00	0.00	0.00	0.00	0.07	0.01	0.13	0.17	0.00	0.00	0.01	0.00	0.00
P$_2$O$_5$	0.00	0.00	0.00	0.00	0.00	0.00	0.11	0.22	0.24	0.00	0.00	0.01	0.00	0.00
Total	85.01	85.15	85.02	85.12	85.10	85.28	84.87	84.96	84.91	86.86	86.67	85.08	84.85	84.95
B $apfu$	3.00	3.00	3.00	3.00	3.00	3.00	3.00	3.00	3.00	3.00	3.00	3.00	3.00	3.00
Si	6.04	5.97	6.01	5.99	6.01	5.97	6.11	5.98	6.00	5.64	5.67	6.00	6.06	6.04
^{IV}Al	0.00	0.03	0.00	0.01	0.00	0.03	0.00	0.02	0.00	0.36	0.33	0.00	0.00	0.00
ΣT	6.00	6.00	6.00	6.00	6.00	6.00	6.00	6.00	6.00	6.00	6.00	6.00	6.00	6.00
Al$_z$	6.00	6.00	6.00	6.00	6.00	6.00	6.00	6.00	6.00	6.00	6.00	6.00	6.00	6.00
Al$_r$	0.58	0.77	0.68	0.68	0.67	0.55	0.53	0.89	0.68	0.00	0.06	0.67	0.91	0.92
Ti	0.00	0.01	0.00	0.00	0.01	0.01	0.00	0.00	0.00	0.02	0.01	0.01	0.01	0.00
Fe	1.69	1.62	1.56	1.48	1.51	1.46	1.51	1.31	0.86	2.73	2.23	1.55	1.53	1.61
Mn	0.12	0.07	0.08	0.03	0.03	0.19	0.13	0.03	0.02	0.10	0.11	0.08	0.19	0.24
Mg	0.39	0.34	0.45	0.69	0.57	0.69	0.40	0.41	1.15	0.74	0.82	0.52	0.08	0.05
ΣY	2.78	2.81	2.77	2.88	2.79	2.90	2.57	2.64	2.71	3.59	3.23	2.83	2.72	2.82
Ca	0.09	0.06	0.10	0.04	0.07	0.07	0.07	0.04	0.03	0.10	0.13	0.07	0.01	0.01
Na	0.50	0.51	0.52	0.52	0.55	0.50	0.74	0.77	0.77	0.50	0.52	0.52	0.36	0.24
K	0.00	0.00	0.00	0.00	0.00	0.02	0.00	0.03	0.04	0.00	0.00	0.00	0.00	0.00
$\square$	0.41	0.43	0.38	0.44	0.38	0.41	0.19	0.16	0.16	0.40	0.35	0.43	0.63	0.75
ΣX	1.00	1.00	1.00	1.00	1.00	1.00	1.00	1.00	1.00	1.00	1.00	1.00	1.00	1.00
Fe#	0.81	0.83	0.78	0.68	0.72	0.68	0.79	0.76	0.43	0.79	0.73	0.75	0.95	0.97
Na#	0.84	0.90	0.84	0.93	0.88	0.88	0.91	0.95	0.96	0.84	0.80	0.88	0.99	0.98
$R1 + R2$	2.80	2.59	2.70	2.75	2.73	2.91	2.85	2.55	2.83	4.17	3.81	2.74	2.18	2.16
$R3$	6.58	6.81	6.68	6.69	6.68	6.60	6.53	6.91	6.68	6.21	6.41	6.68	6.92	6.92

Calculations were carried out with TOURMAL software package (Yavuz 1997). Fe# = Fe/(Fe + Mg), Na# = Na/(Na + Ca), $R1$ = Na +Ca, $R2$ = Fe + Mg + Mn, $R3$ = Al + 1.33*Ti. Column headings: Şebinkarahisar: average composition, $n = 6$. Elba: average composition. (1): Mean Li content 0.33 wt.% (calculated according to stoichiometric constraints). Calif.: California, average composition. (2): Mean Li content of 0.22 wt.%.

but the magnesium (1.37–2.76 wt.% MgO), calcium (0.21–0.53 wt.% CaO), and sodium (1.52–1.70 wt.% Na$_2$O) contents are higher than the foitite samples from California and Elba. The SiO$_2$, Al$_2$O$_3$, TiO$_2$, and FeO contents in these tourmaline localities, however, show similar compositional ranges. Each tourmaline fiber is commonly compositionally zoned along their length, in contrast to the foitite from Elba. These compositional variations may result from the contribution of different types of ore-related solutions in the hydrothermal systems. During the early stages of growth, the fibers generally are poor in iron; the content of iron then increases considerably toward the end of each fiber. Figure 3 shows schematically a typical fiber of foitite with the compositions indicated over the length of the fiber. The

electron-microprobe results of a selected fiber indicate that the Fe, Mn, and Ca increases as crystallization proceeded, whereas P, K, Mg, and Na contents decreased. The Si, Al, and Ti contents, however, do not show much variation.

The chemical composition of foitite fibers is given in Figure 4 in terms of $R1+R2$ versus $R3$. This plot indicates that the composition of the tourmaline corresponds to the ideal alkali-deficient substitution proposed by Foit & Rosenberg (1977). The chemical spectrum of foitite samples shows an important resemblance to the tourmaline from the association of several polymetallic and uranium-bearing deposits in volcanic rocks (Fuchs & Maury 1995). The mean composition of other examples of alkali-deficient tourmaline is given on this figure for

comparison only. The distribution of foitite composi-
tions on a diagram of Fe *versus* Mg shows a great simi-
larity in terms of the schorl trend (Fig. 5). The slope of

the foitite vector, however, is lower than the schorl
trend, possibly because of the lower iron content of
foitite. All the chemical data for the foitite fall within
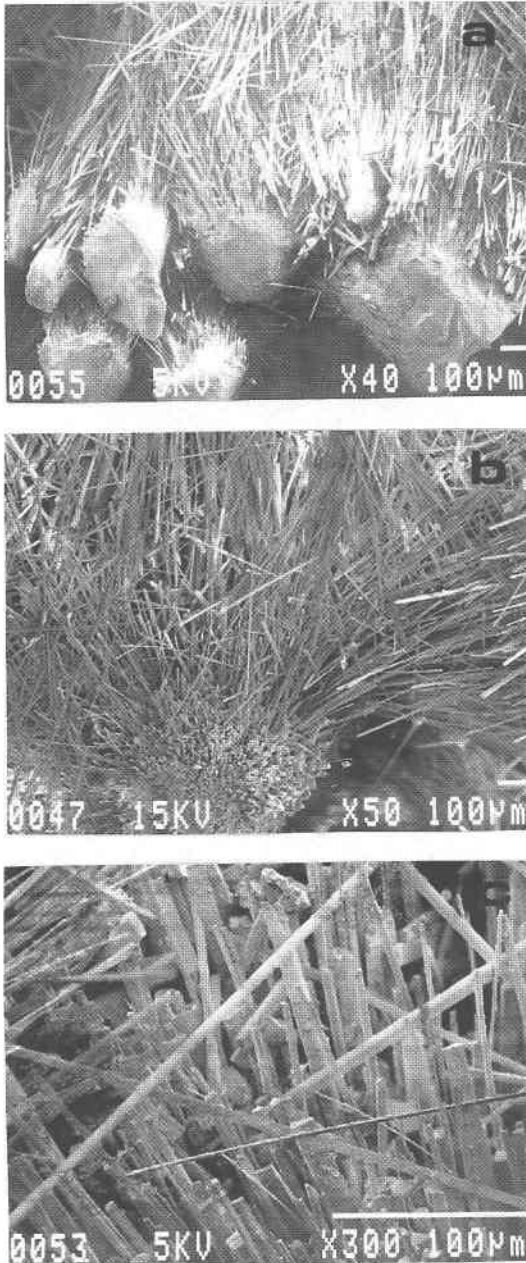the schorl quadrant, with Fe > Mg and Na > Ca (Fig. 6).

FIG. 2.   Scanning electron microphotographs of foitite from
Şebinkarahisar, Giresun. (a) Low-magnification image of
several fibrous patches developed in a cavity in a quartz
vein. (b, c) High-magnification images of acicular foitite
fibers.
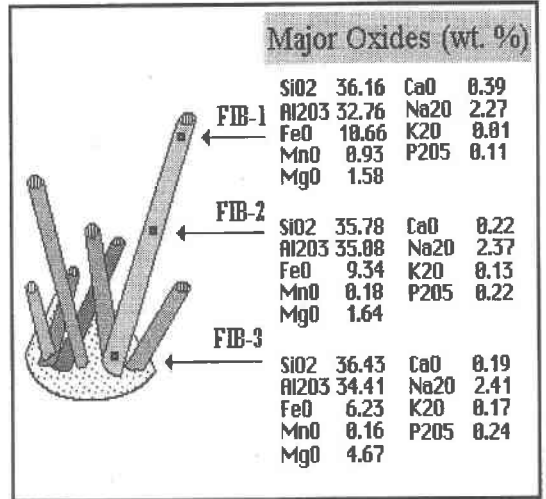
FIG. 3.   Sketch of compositional zoning of a single sample of
fibrous foitite.
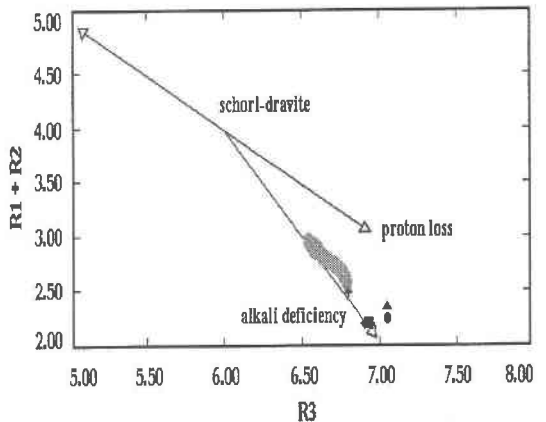
FIG. 4.   Plot of electron-microprobe data on the $R1 + R2$ *ver-
sus* $R3$ diagram. Shaded area: fibrous tourmaline composi-
tion of Şebinkarahisar area, filled box: mean composition
of foitite from southern California (MacDonald *et al.* 1993),
filled diamond: mean composition of fibrous foitite from
Filone della Speranza, Elba (Pezzotta *et al.* 1996), filled
triangle: mean composition of alkali-deficient schorl from
Jack Creek, Montana (Foit *et al.* 1989), filled circle: mean
composition of alkali-deficient schorl from Ben Lomond,
Australia (Foit *et al.* 1989), cross: mean composition of
alkali-deficient tourmaline from Sullivan, British Colum-
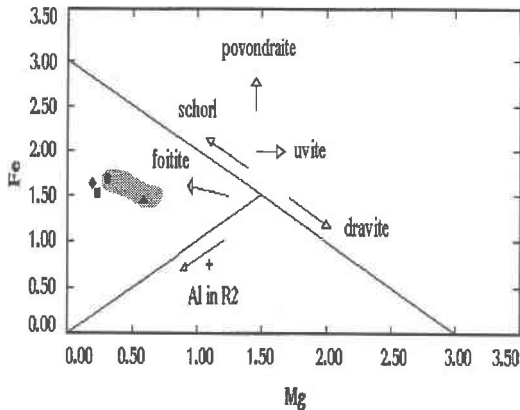bia (Jiang *et al.* 1997).

FIG. 5. Plot of foitite composition together with the selected samples of alkali-deficient tourmaline on Fe *versus* Mg diagram.
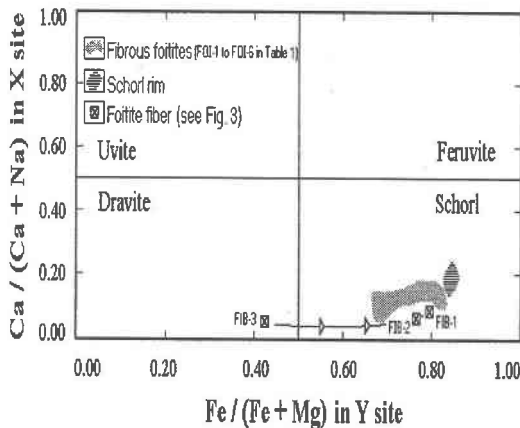

FIG. 6. Plot of Fe/(Fe + Mg) in Y site *versus* Ca/(Ca + Na) in X site of tourmalines.

FIG. 7. a. Fibrous tourmaline compositions from Şebinka-rahisar, Giresun area in terms of Na–Ca–□ diagram, where □ represents a vacancy in the X site. b. Chemical compositions of foitite in terms of $Fe_{(tot)}$–Mg–Al, with compositional trends after Henry & Guidotti (1985).

The schorl rim surrounding the cavities in the quartz veins has a composition similar to that of the fibrous foitite, except for slightly higher Fe and Ca contents. The chemical composition of a fiber in Figure 3 also is included in Figure 6 to document the compositional trend. It is clear from this figure that the starting composition of the solution was Mg-rich. Depending on the increasing fractionation, ore-related solutions were enriched in iron and thus the chemical composition shifted from the dravite to the schorl end member.

The chemical make-up of the X site is shown in a plot in terms of Na–Ca–□ (Fig. 7a). The chemical variation is between the Na and vacancy (*i.e.,* □), with slight increase toward the Na component. In terms of
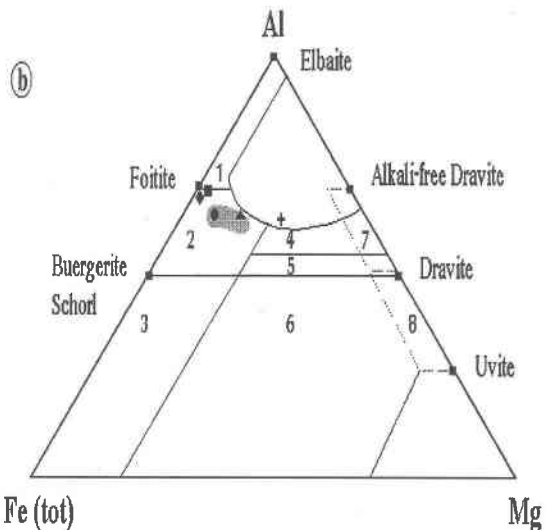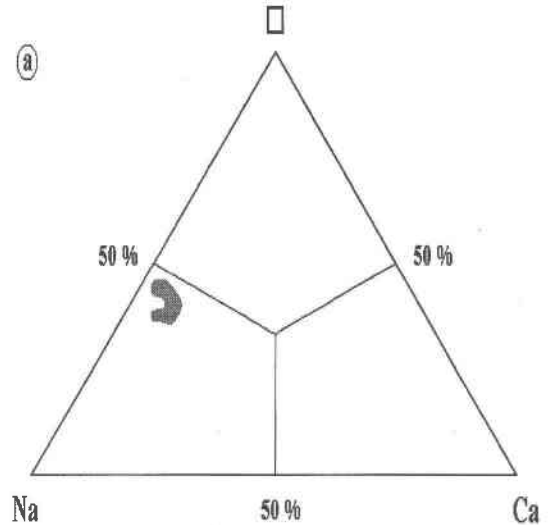
the Fe–Mg–Al diagram (Henry & Guidotti 1985), the compositions of fibrous tourmaline from the Şebinkar-ahisar area plot in field 2 (Fig. 7b), and correspond to tourmaline from Li-poor granites and their associated pegmatites and aplites. The compositional variation of

fibrous foitite from the Şebinkarahisar area is very similar to those of the alkali-deficient schorl from Jack Creek, Montana and Ben Lomond, Australia (Foit *et al.* 1989, Foit 1989).

Using the increasing fractionation *versus* atomic fraction diagram (Jolliff *et al.* 1986), we have observed that among the elements Fe, Mg, Mn, and Ti, Fe and Mg are good indicators of progressive crystallization of foitite compositions (Fig. 8). With increasing fractionation, Mn reaches its maximum and then diminishes as the temperature falls during crystallization. This inference is in agreement with the schematic ideal sequence of crystallization proposed by Jolliff *et al.* (1986). The chemical composition of the foitite fiber in Figure 3 indicates that Mn increases during its crystallization. On the other hand, in a plot of all data on atomic fraction *versus* Fe + Mg diagram (Fig. 8), Mn does not show a clear trend compared those of the Fe and Mg. It makes a distribution similar to parabola, with a peak corresponding to 2.2 Mg + Fe. The different behavior of Mn from Şebinkarahisar area may be used as an index at the crystallization history of foitite in relation to mineralized systems. This conclusion, however, must be checked in further studies of foitite specifically taken from mineralized environments.

The chemical compositions of the foitite samples from Şebinkarahisar are shown on plots of $Na^*_X + Mg^*_Y$ *versus* $\square + Al_Y$ and $Ca_X + Mg^*_Y$ *versus* $Na_X + Al_Y$ diagrams (Figs. 9a, b), where $Mg^* = Mg + Fe + Mn$, $Na^* = Na + K$, $\square = X$-site vacancy. These compositions are characterized by approximately negative linear regression lines, showing the major chemical substitutions: $Na_X + (Fe,Mg)_Y \rightleftharpoons \square_X + Al_Y$ and $Ca_X + (Fe,Mg)_Y \rightleftharpoons Na_X + Al_Y$. These chemical substitutions

are of almost identical to those in the alkali-deficient tourmaline from the Sullivan Pb–Zn–Ag deposit, British Columbia, as given by Jiang *et al.* (1997).

DISCUSSION

The study area is located in the eastern part of Pontide metallogenic belt, which includes abundant Pb–Zn–Cu mineralization. The area produced small- to medium-scale polymetallic mineral deposits. The Asarcık region (Şebinkarahisar, Giresun) was investigated in detail by several researchers because of high background of radioactive anomalies in the magmatic rocks (Çalapkulu 1982). The Pb–Zn–Cu mineralized veins in Upper Cretaceous to Upper Paleocene granitic rocks and E–W- and NE–SW-trending normal faults generally control the emplacement of volcanic rocks. Galena, sphalerite, chalcopyrite, pyrite, arsenopyrite,

Fig. 9. Plots of (a) $\square_X + Al_Y$ *versus* $Na^*_X + Mg^*_Y$, and (b) $Na^*_X + Al_Y$ *versus* $Ca_X + Mg^*_Y$ diagrams showing X- and Y-site subtitutions in foitite, where Na^* represents $Na + K$, and Mg^* represents $Mg + Fe + Mn$ (*apfu*).
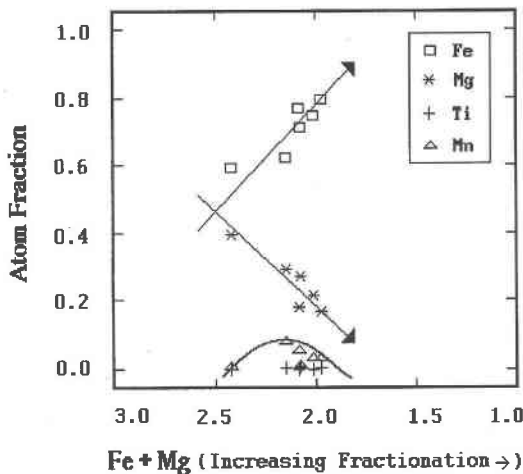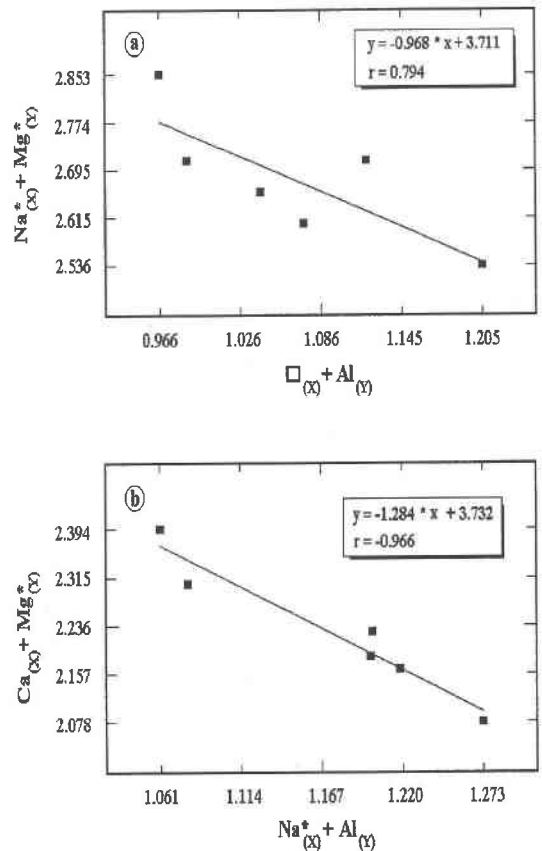
Fig. 8. Compositional trends of fibrous foitite in terms of atom fractions of Fe, Mg, Ti, and Mn *versus* (Fe + Mg) *apfu* after Jolliff *et al.* (1986).

and tetrahedrite constitute the main ore minerals. The associated gangue minerals are quartz, barite, and calcite (Çalapkulu 1982). The chemical composition of black tourmaline in the Şebinkarahisar Pb–Zn–Cu mineralized area varies from dravite to schorl end-members. Tourmaline suns in monzonite and syenite tend to be schorl, whereas black tourmaline associated with Pb–Zn–Cu mineralization in quartz veins approaches dravite (work in progress).

Although the chemical compositions of southern California and Elba foitite samples are similar to ours, their macroscopic appearances and physical properties are different (MacDonald *et al.* 1993, Pezzotta *et al.* 1996). The fibrous foitite described here shows a great similarity in terms of rock composition, physical appearance and mode of occurrence to the fibrous foitite described by Pezzotta *et al.* (1996). Its chemical composition, however, presents an important distinction, especially with respect to the Mn, Mg, Ca, and Na contents. The chemical distinction between the fibrous foitite from Şebinkarahisar and that from Elba possibly resulted from the chemical composition of hydrothermal fluids in the Şebinkarahisar environment of Pb–Zn–Cu mineralization. The behavior of Mn seems to have had an important effect during the crystallization of foitite from the low-temperature ore-bearing solutions.

Mn-rich tourmaline is generally rare. This type of tourmaline is found most commonly in Na–Li-rich granitic pegmatites, with up to 8.86 wt.% MnO contents (Shigley *et al.* 1986). However, alkali-deficient tourmaline in the foitite compositional range contains high levels of Mn (up to 1.71 wt.% MnO) compared to tourmaline compositions belonging to the dravite–schorl solid-solution series. Jiang *et al.* (1997) reported unusually high levels of Mn (up to 1.48 wt.% MnO) in alkali-deficient tourmaline from some of the Sullivan Pb–Zn–Ag deposit. They attributed the presence of Mn-rich alkali-deficient tourmaline to the local availability of Mn and the lack of other coexisting minerals that preferentially incorporate Mn into their structures. We have not observed important Mn-bearing minerals in study area that could buffer the chemical composition of foitite. However, the Mn may be supplied by Mn-rich minerals such as silicate, carbonate or oxide compositions during the formation of foitite in cavities of quartz veins.

ACKNOWLEDGEMENTS

REFERENCES

ÇALAPKULU, F. (1982): *The investigation of Asarcık (Şebinkarahisar–Giresun) uranium-bearing Pb–Zn–Cu mineralization.* Dissertation of Assoc. Professorship (in Turkish), Ege Univ., İzmir, Turkey.

FOIT, F.F., JR. (1989): Crystal chemistry of alkali-deficient schorl and tourmaline structural relationships. *Am. Mineral.* **74**, 422-431.

_____, FUCHS, Y. & MYERS, P.E. (1989): Chemistry of alkali-deficient schorls from two tourmaline – dumortierite deposits. *Am. Mineral.* **74**, 1317-1324.

_____ & ROSENBERG, P.E. (1977): Coupled substitutions in the tourmaline group. *Contrib. Mineral. Petrol.* **62**, 109-127.

FUCHS, Y. & MAURY, R. (1995): Borosilicate alteration associated with U–Mo–Zn and Ag–Au–Zn deposits in volcanic rocks. *Mineral. Deposita* **30**, 449-459.

HENRY, D.J. & GUIDOTTI, C.V. (1985): Tourmaline as a petrogenetic indicator mineral: an example from the staurolite-grade metapelites of NW Maine. *Am. Mineral.* **70**, 1-15.

JIANG, SHAO-YONG, PALMER, M.R. & SLACK, J.F. (1997): Alkali-deficient tourmaline from the Sullivan Pb–Zn–Ag deposit, British Columbia. *Mineral. Mag.* **61**, 853-860.

JOLLIFF, B.L., PAPIKE, J.J. & SHEARER, C.K. (1986): Tourmaline as a recorder of pegmatite evolution: Bob Ingersoll pegmatite, Black Hills, South Dakota. *Am. Mineral.* **71**, 472-500.

MACDONALD, D.J., HAWTHORNE, F.C. & GRICE, J.D. (1993): Foitite, □ [(Fe$^{2+}_2$(Al,Fe^{3+})]Al$_6$Si$_6$O$_{18}$(BO$_3$)$_3$(OH)$_4$, a new alkali-deficient tourmaline: description and crystal structure. *Am. Mineral.* **78**, 1299-1303.

OYMAN, T., DELALOYE, M., PİŞKIN, Ö. & ÇALAPKULU, F. (1995): Petrochemical and K–Ar radiometric investigation of granitoids from Şebinkarahisar area (Giresun–Turkey). *In* International Earth Sciences Colloqium on the Aegean region, İzmir-Güllük, Turkey (Ö. Pişkin, M. Ergün, M.Y. Savaşçın & G. Tarcan, eds.), 429-439.

PEZZOTTA, F., HAWTHORNE, F.C., COOPER, M.A. & TEERTSTRA, D.K. (1996): Fibrous foitite from San Piero in Campo, Elba, Italy. *Can. Mineral.* **34**, 741-744.

SHIGLEY, J.E., KANE, R.E. & MANSON, D.V. (1986): A notable Mn-rich gem elbaite tourmaline and its relationship to "tsilaisite". *Am. Mineral.* **71**, 1214-1216.

YAVUZ, F. (1997): Tourmal: software package for tourmaline, tourmaline-rich rocks and related ore deposits. *Comput. Geosci.* **23**, 947-959.

Received May 23, 1998, revised manuscript accepted November 25, 1998.